SHEAR RELAXATION BEHAVIOUR IN LINEAR REGIME OF DILUTED CARBON NANOTUBE SUSPENSIONS

C. Cruz[1], L. Illoul[1], F. Chinesta[2], G. Régnier[1]*
[1] PIMM, UMR CNRS 8006, Paris, France, [2] EADS Corp. Inter. Chair, ECN, Nantes, France
* Corresponding author (gilles.regnier@paris.ensam.fr)

Keywords: *carbon nanotubes, suspensions, Brownian dynamics, rheology, relaxation*

1 Introduction

Carbon nanotubes (CNT) are very long cylinders formed by rolled-up graphene sheets at the nano scale. In addition to their unique structure, interest for CNTs is based on their impressive physical properties [1]. CNTs have been envisaged as component-material in a large range of applications: electrical circuits, nano-probes for near-field microscopes, high-resolution gas-molecules detectors, drug and gene delivery systems, high-strength fibres and high-performance polymer-based composites. A large number of envisaged applications require dissolving CNTs and processing them in liquid phase. Control of those forming processes needs a deep understanding of the rheology of CNT suspensions [2]. In that context, this work tackles the modelling of the rheological behaviour of dilute and low semi-dilute suspensions of treated CNTs into a Newtonian solvent. CNTs have an important influence on the viscous behaviour of their suspensions. For example, dilute and low semi-dilute suspensions of treated SWNT within an epoxy resin exhibit a strong shear-thinning behaviour. Shear-thinning behaviour has been explained in terms of the competition between two physical phenomena: CNT orientation in the flow direction and CNT random misalignment due to Brownian motion. Shear-thinning signature has been satisfactory modelled by a Fokker Planck simple orientation model, where CNTs are considered as rigid fibres with high aspect ratio (~200) subjected to a homogeneous shear-flow and rotary thermal diffusion [3]. On the other hand, when those suspensions are submitted to a small-amplitude oscillatory deformation test, a mild elasticity is observed. In that case, the intrinsic bending dynamics of CNTs has been proposed to explain such interesting linear viscoelastic response. In fact, a semi-flexible filament model perfectly straight (worm-like chain) is able to reproduce such elastic response under dynamic solicitation [4]. However, CNTs contain defects that form natural bent structures in absence of external forces. Recently, using a semi-flexible filament model with a natural non-straight configuration, it was demonstrated that the dynamic response of a non-straight system differs from that one of a perfectly straight [5]. With the purpose of extent the validity of such CNT model (containing defects), this work is devoted to study numerically the rheological response of a CNT diluted suspension after applying a shear strain-step.

2 Modelling

A treated CNT is represented by a semi-flexible filament model with a non-straight configuration in absence of external forces due to the existence of topological bent defects. The assumption of the natural existence of bent junctions in the CNT structure is justified by two facts: 1) the common apparition of topological defects (for instance, pentagon/heptagon pair defect) during the CNT synthesis [6] that can induce several kinds of curvatures on the CNT structure according to the specific morphology of the localized defect [7], and 2) the experimental evidence obtained by different high-resolution microscopy techniques [8] revealing both the presence of localized junctions on CNT structures and a generalized tortuosity in CNT samples.

For study the rheological response of dilute CNT suspensions a Brownian dynamics (BD) approach is employed. For that reason, the semi-flexible filament model is discretized in a non-freely jointed multi bead-rod model composed of n beads with position $\mathbf{r}_i$, connected by $n - 1$ rods of length a, as showed in Fig. 1. Physical length of the CNT is given by the total length of the chain $(n - 1)a$. Beads are the centres of hydrodynamic resistance and also represent the existence of a structural bent junction.

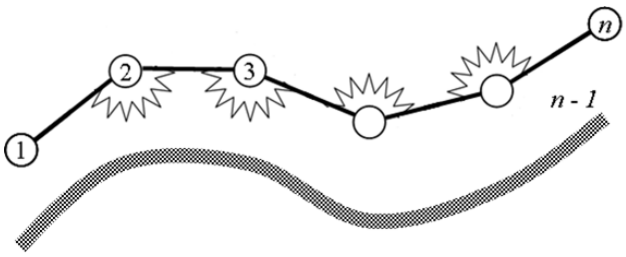

Fig. 1. Non-freely jointed bead rod chain model composed of n beads and n - 1 rods of length a. An equivalent continuous semi-flexible filament is depicted below the discretized model

Constitutive rods are supposed inextensible and natural rod misalignment (i.e. bent structure in absence of external forces) is generated following the next formula:

$$\theta_i^0 = \theta_{i-1}^0 - \Delta\theta^{\max} + U(0,1)\cdot 2\Delta\theta^{\max} \qquad (1)$$

where $\Delta\theta^0{}_i$ is the minimal-bending-energy director angle of rod i, $\Delta\theta^{\max}$ is the maximal misalignment between two consecutive rods and $U(0,1)$ is a continuous uniform random distribution function defined between 0 and 1. An internal bending potential given by the action of a hypothetical flexion spring between each pair of rods is used to capture the bending flexibility of the CNT structure. Current modelling approach supposes also an isotropic friction tensor. In terms of the simulation of a rheological test in the linear regime of a dilute suspension several hypotheses are made: 1) CNTs are embedded into a Newtonian matrix of viscosity η_s, 2) kinematics of the Newtonian matrix is undisturbed by the presence of nanotubes (acceptable assumption in dilute regime and under rheometric flows), 3) applied flow field is considered homogeneous at the scale of the nanotube 4) no physical interactions between CNT exist, 5) hydrodynamic interactions inside the CNT can be omitted and 6) electrostatic, magnetic and gravitational external forces are neglected.

2.1 Mathematical formulation

Kinematics is given from one hand by the resolution of n force balances established on each bead:

$$\mathbf{0} = \mathbf{F}_i^d + \mathbf{F}_i^b + \mathbf{F}_i^\phi - \mathbf{n}_{ij}\boldsymbol{\lambda}_j \qquad (2)$$

where $\mathbf{F}_i^d$ is the hydrodynamic force acting on bead i, $\mathbf{F}_i^b$ is the Brownian force acting on bead i, $\mathbf{F}_i^\Phi$ is the bending potential force acting on bead i, $\boldsymbol{\lambda}_j$ is a tension force associated to the rod j and $\mathbf{n}_{ij}$ is a linear operator that associates a proper unit rod vector to the tension force. On the other hand, n - 1 equations determine the inextensibility of the rods:

$$\dot{\mathbf{r}}_i \cdot \mathbf{u}_i - \dot{\mathbf{r}}_{i+1} \cdot \mathbf{u}_i = 0 \qquad (3)$$

where $\dot{\mathbf{r}}_i$ is the velocity of bead i. Hydrodynamic force $\mathbf{F}_i^d$ writes as follows:

$$\mathbf{F}_i^d = \zeta\left(\mathbf{D}\cdot\mathbf{r}_i - \dot{\mathbf{r}}_i\right) \qquad (4)$$

where ζ is local friction coefficient and $\mathbf{D}$ is the rate-of-strain tensor. The set of Brownian forces follows a Gaussian distribution defined by the next moments:

$$\left\langle \mathbf{F}_i^b(t) \right\rangle = \mathbf{0} \qquad (5)$$

$$\left\langle \mathbf{F}_i^b(t) \otimes \mathbf{F}_j^b(t') \right\rangle = \frac{2\zeta k_B T}{\Delta t}\mathbf{I} \qquad (6)$$

where k_B is the Boltzmann constant, T is the absolute temperature, Δt is the time step of the simulation and $\mathbf{I}$ is the identity matrix. In accord with the worm-like chain model for semi-flexible polymers [4], the internal bending potential can be redefined for a bead-rod chain model with non-straight minimal bending-energy configuration as follows:

$$\phi = -\frac{K_b}{a}\sum_{i=2}^{n-1}\mathbf{Z}_i\mathbf{u}_i \cdot \mathbf{u}_{i-1} \qquad (7)$$

where K_b is a rigidity constant, $\mathbf{Z}_i$ is a linear operator that counter-rotates vector $\mathbf{u}_i$ of $\Delta\theta^0{}_{i,i\text{-}1}$ (internal angle between $\mathbf{u}_i$ and $\mathbf{u}_{i\text{-}1}$ in the absence of external forces). In summary, using the n equations given in (2) plus the n - 1 equations given in (3) a linear system of equations describing the motion of the bead-rod chain model can be established, where the unknown variables are n instantaneous bead velocities $\partial\mathbf{r}_i/\partial t$ plus n - 1 rod tensions λ_j. Position of the bead-rod chain model at the end of each time step is obtained using the bead velocities calculated at the beginning of the respective time step by using a first-order integration scheme. Such single-step algorithm is coherent with the explicit corrector-predictor integration scheme [10] given the fact that the velocity of each rod during an entire time step is always perpendicular to its orientation (rod length is always guaranteed).

In order to quantify the shear stress contribution coming from the suspended particles (i.e. CNTs represented as non-freely jointed bead-rod chains), we resort to the classical Kramers-Kirkwood expression for coarse-grained models in kinetic theory:

$$\boldsymbol{\tau}_p = c\sum_v \left\langle \mathbf{R}_v \otimes \mathbf{F}_v^{(d)} \right\rangle \qquad (8)$$

where c is the number of density of suspended particles and $\mathbf{R}_v = \mathbf{r}_v - \mathbf{r}_c$ is the relative location of bead v to the centre of mass of the multi bead-rod chain $\mathbf{r}_c$. Previous expression (8) is implemented into the BD algorithm using a semi-implicit scheme that weight up properly the instantaneous Brownian forces generated at the beginning of time step through the respective entire Δt.

2.2 BD implementation

Previous modelling was already validated in front of the linear viscoelastic dynamic response of a freely-jointed (three-bead) (two-rod) system using a bi-dimensional BD simulation [5]. Hence, for the sake of reducing computational times, BD simulation of the shear-strain step test is also implemented in a bi-dimensional Cartesian framework. A BD population of 5000 chains is used in all simulations. In order to guarantee convergence to the central values for the implemented first-order integration scheme a time step $\Delta t = \lambda_{bead}/10^{-5}$ (where λ_{bead} is the bead diffusion time) is the minimal requirement.

All numerical rheological tests are executed on a BD population equilibrated in temperature. Thermal equilibrium state is obtained from a BD simulation with no external flow until one of two criteria is satisfied: stabilization of the stored internal-bending energy or integration during three times the longest characteristic time of the chain model. Characteristic time of the current chain model is given by the rotational diffusion time of an equal-length multibead rigid-rod system containing n beads:

$$\lambda_n = \frac{\zeta L^2 n(n+1)}{72(n-1)k_B T} \qquad (9)$$

where L is the total length of the chain. Once an equilibrium configuration has been reached for the BD population, a shear-strain function $\gamma=\gamma'_0 t$ is applied. During the shear-strain step a constant shear-strain rate γ'_0 is imposed during a charging time t_c and the BD-calculated shear-stress and internal bending-energy signals are stored. Shear-strain at the end of the shear-strain step, i.e. $\gamma_0=\gamma'_0 t_c$ is always chosen inside the linear regime. On the other hand, with the aim to closely mimic the rapid strain-rates imposed experimentally, the constant shear-rate implemented in the BD simulations is calculated using a shearing time shorter than the period associated with a reciprocal frequency $\omega_R=\omega\lambda_n=10^3$. Once charging time is ended, shearing is stopped and the BD system is let to relax. BD-calculated shear-stress and internal-energy signals are stored in function of time until at least one of two criteria is satisfied: stabilization of the stored internal bending-energy during one-half of the longest characteristic time of the current chain model or integration during three times the same longest characteristic time.

3 Simulation results

In general, under the current strain-rate conditions, multi bead-rod chains exhibit a shear-stress modulus vanishing practically instantaneously. However, despite the extremely rapid relaxation, freely-jointed systems behave differently with respect to the non-freely jointed ones, as observed in the shear-stress and internal bending-energy curves showed in Fig. 1 and Fig. 2 respectively for several two-rod systems.

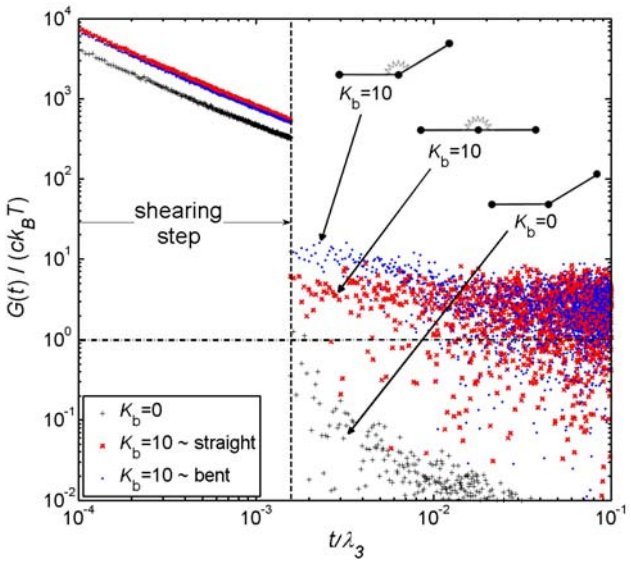

Fig. 1. Shear-stress modulus during a shear-strain step test for different (two-rod) systems: freely jointed and two non-freely jointed ones (straight and bent configurations)

In Fig. 1 can be appreciated a drop of the shear-modulus in almost three orders of magnitude for the freely-jointed system and a smaller drop of approximately two orders of magnitude for the non-freely jointed systems. This preponderant viscous character is found in agreement with the linear viscoelastic response in dynamic mode [5]. Differences between the straight and bent non-freely jointed systems are blurred by the stochastic noise in Fig. 1, but a more clear distinction can be made on Fig. 2 where the natural bent system exhibits a relaxation time that is almost twofold that one of the natural straight model. That difference appears consistent with the larger values of shear-modulus exhibited by the natural bent system during the first transition times in Fig. 1.

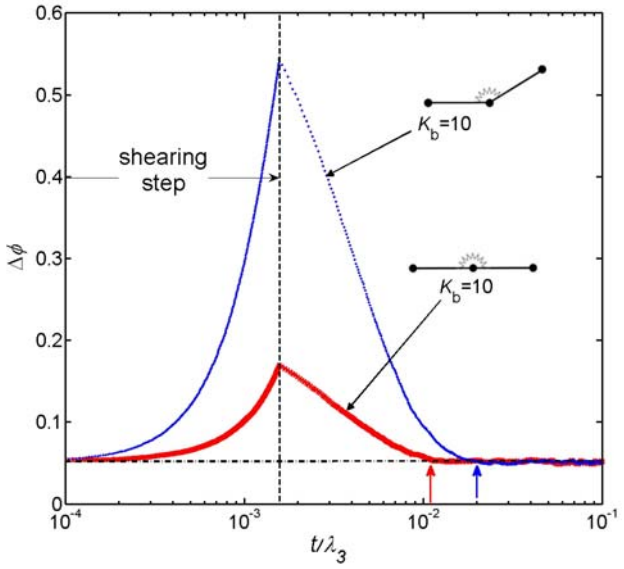

Fig. 2. Change in bending-energy during a shear strain step test for two non-freely jointed (two-rod) systems: straight and bent configurations

Bending rigidity is found to play an important role in the relaxation signature of the non-freely jointed systems with natural bent configuration as observed in Fig. 3. On one hand, stored bending energy during the shearing step is related directly to the bending rigidity constant K_b. On the other hand, as higher is the bending rigidity shorter is the relaxation time associated with. This fact explains why higher solicitation frequencies are required for activating the mild elasticity in the linear dynamic tests as the bending rigidity constant of the chain is enhanced [5].

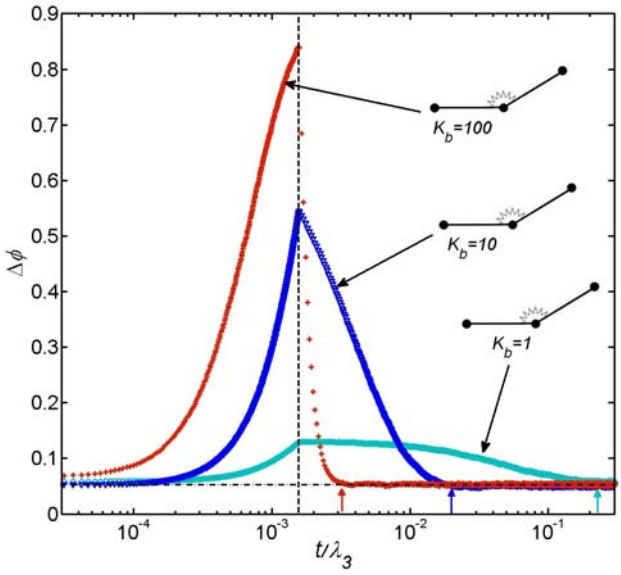

Fig. 3. Internal bending-energy during a shear strain step test for three naturally bent (two-rod) chains with different bending rigidity constant

In addition, the number of constitutive rods is showed to be also a determinant parameter in the relaxation behaviour of non-freely jointed multi bead-rod systems in dilute solution. Differences in the energy-relaxation spectra by varying the number of rods are coherent with the dynamic response presented elsewhere [5].

Finally, for evaluating the performance of the coarse-grained CNT model, the shear-stress experimental data after a shear-strain step applied on a 0.1 wt.% treated SWNT suspension are compared in Fig. 4 with the predicted shear-stress evolution obtained from a BD simulation fed with real physical parameters. BD simulation parameters are calculated for a mono-disperse population of HiPco (High Pressure CO Conversion) treated SWNTs (L=400nm, diameter d=1nm, ρ=1.45g/cm^3) mimicked by chain models constituted by 4 rods (n=5) and exhibiting a persistence length L_p=138μm. Persistence length L_p relates the bending rigidity with the temperature ($L_p = K_b / k_B$T). The value of persistence length employed in our simulations corresponds to the upper limit of the interval identified experimentally for those kinds of nanotubes. We suggest that this fact can be related to the local stiffness of a bent junction in the CNT structure ($\Delta\theta^{max} \leq 30°$). On the other hand, suspending medium (pre-epoxy resin) is

characterised by a viscosity η_s=10Pa s and a density ρ_s = 1.16g/cm^3.

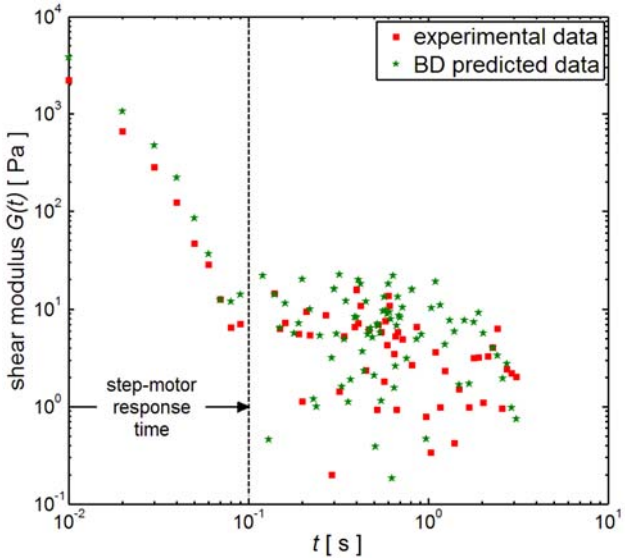

Fig. 4. Comparison between the experimental and the BD-predicted shear modulus relaxation of a 0.1wt.% SWNT suspended within a pre-epoxy resin

In spite of the BD simulation overestimates the evolution of the shear modulus during the early times after the shearing step (0.01s to ~0.06s), a direct comparison is only feasible after the step-motor response time (marked by a vertical dashed line in Fig. 4), which guarantees absolute confidence on the values recovered by the rheometer. Interestingly, after the motor response time, BD-prediction and simulation are statistically comparable.

4 Conclusions

Individual treated CNTs in suspension have been modelled as non-freely jointed multi bead-rod chains with an intrinsic bent configuration due to the natural existence of topological defects in the CNT structure. BD-simulated shear-stress evolution after a linear shear-strain step have been found coherent with the rheological responses obtained under dynamic solicitation [5], proving the consistency of the CNT coarse-grained model in the framework of linear viscoelasticity. The quasi-instantaneous relaxation of shear-stress after shearing-step is consistent with the non-zero limiting viscosity obtained in the dynamic response at high frequencies. In addition, relaxation time of the stored bending energy after a shear-strain step shortens as the bending rigidity constant increases. Finally, real shear-strain step tests on dilute and semi-dilute suspensions of treated SWNTs within a pre-epoxy resin exhibit a rheological behaviour in agreement with the BD-simulated shear-strain step tests on dilute solutions of non-freely jointed bead-rod chains with natural bent configuration.

References

[1] R.S. Ruoff, D. Qian and W.K. Liu. “Mechanical properties of carbon nanotubes: theoretical predictions and experimental measurements”. *Physique*, Vol. 4, pp 903-1008, 2003.

[2] S.B. Kharchenko, J.F. Douglas, J. Obrzut, E.A. Grulke and K.B. Migler “Flow-induced properties of nanotube-filled polymer materials”. *Nature Materials*, Vol. 3, pp 564-568, 2004.

[3] A.W.K. Ma, F. Chinesta and M.R. Mackley. “The rheology and modeling of chemically treated carbon nanotubes suspensions”. *Journal of Rheology*, Vol. 53, No. 3, pp 547-573, 2009.

[4] V. Shankar, M. Pasquali and D.C. Morse. “Theory of linear viscoelasticity of semiflexible rods in dilute solution”. *Journal of Rheology*, Vol. 46, No. 5, pp 1111-1154, 2002.

[5] C. Cruz, L. Illoul, F. Chinesta and G. Régnier. “Effects of a bent structure on the linear viscoelastic response of diluted carbon nanotube suspensions”. *Rheologica Acta*, Vol. 49, No. 11, pp 1141-1155, 2010.

[6] S. Lijima, T. Ichihashi and Y. Ando. “Pentagons, heptagons and negative curvature in graphite microtubule growth”. *Nature*, Vol. 356, No. 6372, pp 776-778, 1992.

[7] K. Wako, T. Oda, M. Tachibana and K. Kojima. “Bending deformation of single-walled carbon nanotubes caused by 5-7 pair couple defect”. *Japanese Journal of Applied Physics 1*, Vol. 47, No. 8, pp 6601-6605, 2008.

[8] A. Vijayaraghavan, C.W. Marquardt, S. Dehm, F. Hennrich and R. Krupke. “Imaging defects and junctions in single-walled carbon nanotubes by voltage-contrast scanning electron microscopy”. *Carbon*, Vol. 48, pp 494-500, 2010.

[9] D.C. Morse. “Viscoelasticity of concentrated isotropic solutions of semiflexible polymers. 1. Model and stress tensor”. *Macromolecules*, Vol. 31, No. 20, pp 7030-7043, 1998.

[10] T.W. Liu. “Flexible polymer chain dynamics and rheological properties in steady flows”. *Journal of Chemical Physics*, Vol. 90, No. 5, pp 826-5842, 1989.